



Synthesis and characterisation of Group 6 metal carbonyl complexes of bis(ferrocenylchalcogeno)propanes: X-ray crystal structures of $[\text{Cr}(\text{CO})_4\{\text{FcTe}(\text{CH}_2)_3\text{TeFc}\}]$, $[\text{Mo}(\text{CO})_4\{\text{FcE}(\text{CH}_2)_3\text{E}'\text{Fc}\}]$ ($\text{E} = \text{E}' = \text{Se}$; $\text{E} = \text{Se}$, $\text{E}' = \text{Te}$; $\text{E} = \text{E}' = \text{Te}$), and $[\text{W}(\text{CO})_4\{\text{FcTe}(\text{CH}_2)_3\text{TeFc}\}]$ ($\text{Fc} = [\text{Fe}(\eta^5\text{-C}_5\text{H}_5)(\eta^5\text{-C}_5\text{H}_4)]$)

Su Jing^{a,1}, Christopher P. Morley^{a,*}, Christopher A. Webster^{a,b}, Massimo Di Vaira^b

^a Department of Chemistry, University of Wales Swansea, Singleton Park, Swansea SA2 8PP, UK

^b Dipartimento di Chimica, Università degli Studi di Firenze, Via della Lastruccia 3, 50019 Sesto Fiorentino (FI), Italy

ARTICLE INFO

Article history:

Received 22 January 2008

Received in revised form 28 March 2008

Accepted 3 April 2008

Available online 7 April 2008

Keywords:

Group 6 metals
Carbonyl complexes
Selenium
Tellurium
Ferrocene
Cyclic voltammetry

ABSTRACT

The Group 6 metal tetracarbonyl complexes $[\text{Cr}(\text{CO})_4\{\text{FcTe}(\text{CH}_2)_3\text{TeFc}\}]$, $[\text{Mo}(\text{CO})_4\{\text{FcE}(\text{CH}_2)_3\text{E}'\text{Fc}\}]$ ($\text{E} = \text{E}' = \text{Se}$; $\text{E} = \text{Se}$, $\text{E}' = \text{Te}$; $\text{E} = \text{E}' = \text{Te}$), and $[\text{W}(\text{CO})_4\{\text{FcTe}(\text{CH}_2)_3\text{TeFc}\}]$ ($\text{Fc} = [\text{Fe}(\eta^5\text{-C}_5\text{H}_5)(\eta^5\text{-C}_5\text{H}_4)]$) have been prepared and fully characterised. Electronic communication between the ferrocenyl groups is observed in the case of $[\text{Mo}(\text{CO})_4\{\text{FcSe}(\text{CH}_2)_3\text{SeFc}\}]$, where the through-bond $\text{Fe}\cdots\text{Fe}$ distance is 13.17 Å, but in the other four complexes the longer through-bond $\text{Fe}\cdots\text{Fe}$ distances (≥ 13.56 Å) preclude it.

© 2008 Elsevier B.V. All rights reserved.

1. Introduction

We have previously reported the synthesis and characterisation of a number of bis(ferrocenylchalcogeno)alkanes [1]. Electronic interaction between ferrocenyl groups was studied in the palladium and platinum complexes of the bis(ferrocenylchalcogeno)propanes, in which communication occurred at through-bond $\text{Fe}\cdots\text{Fe}$ distances below a threshold in the range of 13.17–13.37 Å [2]. As the known chemistry of analogous bidentate ligands having selenium and/or tellurium donor atoms includes coordination to low-valent metal and organometallic species [3–15], we have now synthesized and studied the Group 6 metal carbonyl complexes of the bis(ferrocenylchalcogeno)propanes.

2. Results and discussion

2.1. Synthesis

The syntheses of the Group 6 carbonyl complexes of the bidentate ligands $\text{FcE}(\text{CH}_2)_3\text{E}'\text{Fc}$ (E and $\text{E}' = \text{Se}$ or Te) were straightfor-

* Corresponding author. Present address: School of Chemistry, Cardiff University, P.O. Box 912, Cardiff CF10 3AT, UK. Tel.: +44 2920 879183; fax: +44 2920 874030. E-mail address: morleycp@cardiff.ac.uk (C.P. Morley).

¹ Present address: School of Science, Nanjing University of Technology, Nanjing 210009, PR China.

ward in the cases of $[\text{Cr}(\text{CO})_4\{\text{FcTe}(\text{CH}_2)_3\text{TeFc}\}]$, $[\text{Mo}(\text{CO})_4\{\text{FcE}(\text{CH}_2)_3\text{E}'\text{Fc}\}]$ ($\text{E} = \text{E}' = \text{Se}$; $\text{E} = \text{Se}$, $\text{E}' = \text{Te}$; $\text{E} = \text{E}' = \text{Te}$), and $[\text{W}(\text{CO})_4\{\text{FcTe}(\text{CH}_2)_3\text{TeFc}\}]$, using reactions of the ligand $\text{FcE}(\text{CH}_2)_3\text{E}'\text{Fc}$ with $[\text{M}(\text{CO})_4(\text{nb})]$ ($\text{M} = \text{Cr}$ or Mo ; $\text{nb} = \text{norbornadiene}$) or $[\text{W}(\text{CO})_4(\text{TMPDA})]$ ($\text{TMPDA} = \text{tetramethylpropylenediamine}$) in toluene. Attempts using the same procedure to synthesise $[\text{Cr}(\text{CO})_4\{\text{FcSe}(\text{CH}_2)_3\text{SeFc}\}]$, $[\text{Cr}(\text{CO})_4\{\text{FcSe}(\text{CH}_2)_3\text{TeFc}\}]$, $[\text{W}(\text{CO})_4\{\text{FcSe}(\text{CH}_2)_3\text{SeFc}\}]$ and $[\text{W}(\text{CO})_4\{\text{FcSe}(\text{CH}_2)_3\text{TeFc}\}]$ failed, however, with infrared spectra of the reaction mixtures showing only the presence of starting materials. The observation that analogous complexes of the methyl- and phenyl-substituted ligands $\text{RE}(\text{CH}_2)_3\text{ER}$ ($\text{E} = \text{Se}$ or Te ; $\text{R} = \text{Me}$ or Ph) have previously been prepared in this way [11] may imply lower stability for the complexes of the ferrocenyl-substituted ligands, possibly as a result of increased steric congestion.

The brown complexes obtained are air-stable in the solid state. They are poorly soluble in hydrocarbons, but soluble in chlorocarbon solvents with slow decomposition. The FAB mass spectra showed a parent ion, and occasionally the fragments corresponding to sequential carbonyl loss could be observed. The results of elemental analysis were variable, presumably as a result of ligand dissociation, and good agreement with expected values was only obtained in the case of the two most stable complexes $[\text{Mo}(\text{CO})_4\{\text{FcE}(\text{CH}_2)_3\text{E}'\text{Fc}\}]$ ($\text{E} = \text{Se}$, $\text{E}' = \text{Te}$; $\text{E} = \text{E}' = \text{Te}$).

2.2. NMR spectroscopy

There are two possible intramolecular fluxional processes in these complexes: pyramidal inversion of the coordinated chalcogen atoms, and reversal of the conformation of the hydrocarbon bridge in the chelate ring. If either process (or both processes) is slow on the NMR timescale, four configurational isomers can exist: *meso*-1, *meso*-2 and a degenerate DL pair. Normally the ring reversal process is rapid due to the low torsional barriers associated with M–E bonds, but the rate of pyramidal inversion is strongly dependent on the nature of the chalcogen and the transition metal. The *meso*-2 structure is not favoured due to the high steric crowding. Two sets of signals will therefore be observed when pyramidal inversion is slow: an intense set for the degenerate DL pair and a weaker set for *meso*-1 [7]. Previous studies have shown that for dichalcogenoether complexes of $M(\text{CO})_4$ fragments, the energy barriers to inversion have the sequence: $\text{Te} > \text{Se} > \text{S}$ and $\text{W} > \text{Cr} > \text{Mo}$ [11,16]. The ^1H spectra of $[\text{Mo}(\text{CO})_4\{\text{FcTe}(\text{CH}_2)_3\text{TeFc}\}]$ and $[\text{Mo}(\text{CO})_4\{\text{FcSe}(\text{CH}_2)_3\text{SeFc}\}]$ show resonances for both invertomers consistent with relatively high inversion barriers. The spectrum of $[\text{Mo}(\text{CO})_4\{\text{FcSe}(\text{CH}_2)_3\text{TeFc}\}]$ is very complicated due to the mixed Se/Te ligand. Four isomers may exist as shown in Fig. 1.

In the ^{13}C NMR spectra, when inversion is rapid on the ^{13}C NMR timescale, there will appear to be only two CO environments: CO groups *trans* to a CO group; and CO groups *trans* to a chalcogen atom. Slow inversion will afford five resonances: two for CO groups *trans* to a chalcogen atom in the *meso* and DL invertomers, one for CO groups *trans* to a CO in the DL form, and another two for CO groups *trans* to a CO in the *meso* form. Sometimes only four resonances can be observed due to the coincidence of the chemical shifts of CO groups *trans* to a chalcogen atom in the two invertomers [11]. The ^{13}C NMR spectra of $[\text{Mo}(\text{CO})_4\{\text{FcSe}(\text{CH}_2)_3\text{SeFc}\}]$, $[\text{Mo}(\text{CO})_4\{\text{FcTe}(\text{CH}_2)_3\text{TeFc}\}]$ and $[\text{W}(\text{CO})_4\{\text{FcTe}(\text{CH}_2)_3\text{TeFc}\}]$ only exhibit two CO resonances, which means that the pyramidal inversion is faster than in $[\text{M}(\text{CO})_4\{\text{RTe}(\text{CH}_2)_3\text{TeR}\}]$ ($\text{M} = \text{Cr}, \text{Mo}, \text{W}$; $\text{R} = \text{Me}, \text{Ph}$) [10]. The ^{13}C NMR spectrum of $[\text{Mo}(\text{CO})_4\{\text{FcSe}(\text{CH}_2)_3\text{TeFc}\}]$ shows four CO resonances, which is in accordance with the ^1H spectrum. That of $[\text{Cr}(\text{CO})_4\{\text{FcTe}(\text{CH}_2)_3\text{TeFc}\}]$ appears to show only one CO resonance, but the signal-to-noise ratio of the spectrum was poor.

The ^{125}Te chemical shifts of Group 6 metal complexes generally decrease in the sequence $\text{Cr} > \text{Mo} > \text{W}$ for the same ligand [11]. The ^{125}Te chemical shift of the free ligand $\text{FcTe}(\text{CH}_2)_3\text{TeFc}$ is 299 ppm in CD_2Cl_2 , similar to that in CDCl_3 [1]. After complexation, the values of $\delta(^{125}\text{Te})$ are 429 ppm for $[\text{Cr}(\text{CO})_4\{\text{FcTe}(\text{CH}_2)_3\text{TeFc}\}]$, 344 ppm for $[\text{Mo}(\text{CO})_4\{\text{FcTe}(\text{CH}_2)_3\text{TeFc}\}]$ and 272, 269 ppm for $[\text{W}(\text{CO})_4\{\text{FcTe}(\text{CH}_2)_3\text{TeFc}\}]$, in good agreement with the results for $[\text{M}(\text{CO})_4\{\text{R-Te}(\text{CH}_2)_3\text{TeR}\}]$ ($\text{M} = \text{Cr}, \text{Mo}, \text{W}$; $\text{R} = \text{Me}, \text{Ph}$) [11]. It was possible to measure a W–Te coupling constant (74 Hz) for the first time in DL- $[\text{W}(\text{CO})_4\{\text{FcTe}(\text{CH}_2)_3\text{TeFc}\}]$ due to the high intensity of the signal, but the *meso* signal was too weak for its satellites to be resolved; the same phenomenon has been observed for $[\text{W}(\text{CO})_4\{\text{FcTe}(\text{CH}_2)_3\text{TeFc}\}]$ [7]. The two ^{125}Te resonances of $[\text{W}(\text{CO})_4\{\text{FcSe}(\text{CH}_2)_3\text{TeFc}\}]$ are an indication of the larger inversion energy barrier for the tungsten complex.

The ^{77}Se chemical shifts of $[\text{Mo}(\text{CO})_4\{\text{FcSe}(\text{CH}_2)_3\text{SeFc}\}]$ and $[\text{Mo}(\text{CO})_4\{\text{FcSe}(\text{CH}_2)_3\text{TeFc}\}]$ are similar at around 175 ppm, a shift of only 10 ppm to high field compared to the free ligands.

2.3. X-ray crystallography

Crystals of all five of the new complexes, $[\text{Cr}(\text{CO})_4\{\text{FcTe}(\text{CH}_2)_3\text{-TeFc}\}]$, $[\text{Mo}(\text{CO})_4\{\text{FcE}(\text{CH}_2)_3\text{E'Fc}\}]$ ($\text{E} = \text{E}' = \text{Se}$; $\text{E} = \text{Se}, \text{E}' = \text{Te}$; $\text{E} = \text{E}' = \text{Te}$), and $[\text{W}(\text{CO})_4\{\text{FcTe}(\text{CH}_2)_3\text{TeFc}\}]$, were grown as orange plates by slow evaporation from CH_2Cl_2 /hexanes. They crystallize in the monoclinic crystal system and the space group $P2_1/c$, with one molecule in the asymmetric unit (and no solvent molecule). Selected bond lengths and angles are listed in Table 1.

As an example, the molecular structure of $[\text{Mo}(\text{CO})_4\{\text{FcSe}(\text{CH}_2)_3\text{-SeFc}\}]$ is shown in Fig. 2. The structure reveals the expected *cis*-substituted octahedron about Mo, with a Se–Mo–Se angle of $86.51(2)^\circ$. The range of the iron-carbon distances in the cyclopentadienyl rings (2.003–2.045 Å) is within that expected for ferrocenyl compounds. The ferrocenyl (sp^2) C–Se bond distances are 1.900(4) and 1.893(4) Å, slightly shorter than those in $[\text{Pd}\{\text{FcSe}(\text{CH}_2)_3\text{SeFc}\}_2](\text{PF}_6)_2$ (1.909(4) and 1.901(4) Å) and $[\text{Pt}\{\text{FcSe}(\text{CH}_2)_3\text{-SeFc}\}_2](\text{PF}_6)_2$ (1.910(6) and 1.894(5) Å), but still longer than in the free ligand $\text{FcSe}(\text{CH}_2)_3\text{SeFc}$ (1.872(6) and 1.878(6) Å) [2]. The results are in accordance with the weaker electron-withdrawing strength of the Mo(0) centre compared to that of Pd(II) or Pt(II). On the other hand, the sp^3 C–Se bond distances (1.956(4) and 1.973(4) Å) are shorter than in the free ligand $\text{FcSe}(\text{CH}_2)_3\text{SeFc}$ (1.995(6) and 1.979(6) Å), by slightly larger amounts than were observed in the structures of $[\text{Pd}\{\text{FcSe}(\text{CH}_2)_3\text{SeFc}\}_2](\text{PF}_6)_2$ and $[\text{Pt}\{\text{FcSe}(\text{CH}_2)_3\text{SeFc}\}_2](\text{PF}_6)_2$.

The ligand adopts the DL conformation with Mo–Se 2.6649(7) Å, 2.6751(7) Å, Mo– C_{cisSe} 1.999(5), 2.033(5) Å and Mo– $\text{C}_{\text{transSe}}$ 1.941(5), 1.957(5) Å, so the equatorial M–C bonds *trans* to the Mo–E bonds are significantly shorter than the two axial Mo–C bonds, reflecting the fact that the two Mo–E bonds result in more electron density being available for back-bonding to the two equa-

Table 1

Selected bond lengths (Å) and angles ($^\circ$) for $[\text{M}(\text{CO})_4\{\text{FcE}(\text{CH}_2)_3\text{E'Fc}\}]$ ($\text{M} = \text{Cr}$ or W , $\text{E} = \text{E}' = \text{Te}$; $\text{M} = \text{Mo}$, E and $\text{E}' = \text{Se}$ or Te)

M	Cr	Mo	Mo ^a	Mo	W
E	Te	Se	Se	Te	Te
E'	Te	Se	Te	Te	Te
M–E1	2.6555(7)	2.6649(7)	2.7546(5)	2.7988(8)	2.7903(7)
M–E2	2.6661(7)	2.6751(7)	2.7467(5)	2.8093(8)	2.8013(4)
M–C1	1.870(5)	1.999(5)	2.007(5)	2.009(5)	2.006(7)
M–C2	1.893(5)	2.033(5)	2.044(5)	2.041(5)	2.039(6)
M–C3	1.818(5)	1.941(5)	1.943(5)	1.943(5)	1.943(6)
M–C4	1.836(5)	1.957(5)	1.964(4)	1.969(4)	1.967(6)
C1–O1	1.154(5)	1.141(5)	1.146(6)	1.146(5)	1.151(7)
C2–O2	1.140(6)	1.132(5)	1.141(6)	1.143(5)	1.137(7)
C3–O3	1.160(6)	1.143(5)	1.156(6)	1.155(5)	1.157(7)
C4–O4	1.157(5)	1.147(5)	1.153(5)	1.156(5)	1.153(6)
E1–M–E2	88.75(2)	86.51(2)	87.24(1)	87.46(3)	87.48(1)

^a For $[\text{Mo}(\text{CO})_4\{\text{FcSe}(\text{CH}_2)_3\text{TeFc}\}]$, E1 = Se, E2 = Te.

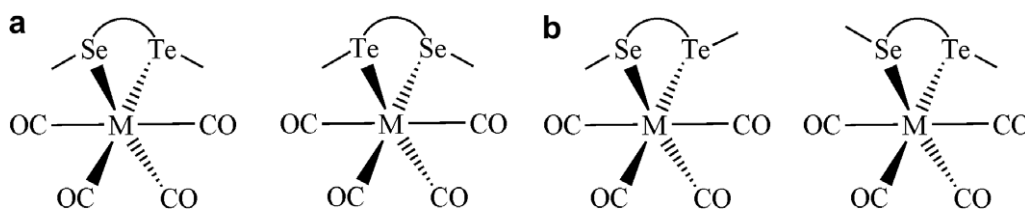


Fig. 1. (a) *meso*- and (b) DL-invertomers of $[\text{Mo}(\text{CO})_4\{\text{FcSe}(\text{CH}_2)_3\text{TeFc}\}]$.

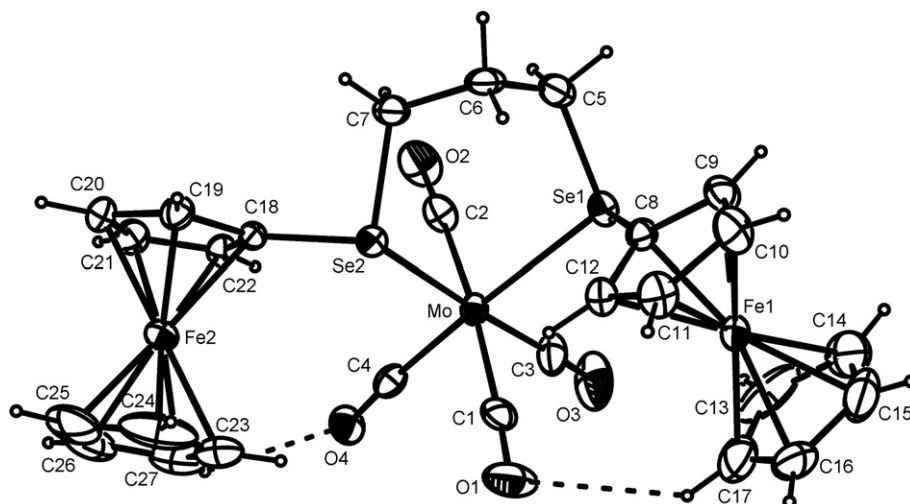


Fig. 2. Structure of $[\text{Mo}(\text{CO})_4\{\text{FcSe}(\text{CH}_2)_3\text{SeFc}\}]$ with 30% probability ellipsoids and atom numbering scheme. The intramolecular contacts affecting two carbonyls (see text) are shown.

torial carbonyls. The same phenomenon is observed for the structures of the other complexes and will be discussed in more detail later.

The refinement of the structure of $[\text{Mo}(\text{CO})_4\{\text{FcSe}(\text{CH}_2)_3\text{TeFc}\}]$ was quite sensitive to the assignment of the Se/Te positions. Actually, the ligand is disorderly oriented, with a slight preference of Te for the site (Te1) which forms the comparatively longer distance to the metal and, obviously, with preference of Se for the other coordination site.

The arrangement of the carbonyl groups in these structures is linear. However, the $\text{M}-\text{C}1-\text{O}1$ and $\text{M}-\text{C}4-\text{O}4$ angles, with values in the range $175.3\text{--}177.2^\circ$, deviate from the idealized 180° value more than do the angles (in the range $177.4\text{--}179.4^\circ$) formed by the other two carbonyls. This may be attributed to short intramolecular $\text{O}\cdots\text{H}$ contacts, in the range $2.652\text{--}2.787\text{ \AA}$, formed by the atoms O1 and O4 in all structures.

It may also be noted that in these structures the direction of the best line through the positions of an E donor atom of the metal and those of the atoms of the *trans* carbonyl is almost parallel to the plane of the vicinal cyclopentadienyl ring. In particular, the absolute values of torsion angles like those through the atoms Mo, Se1, C8 and C12 or through Mo, Se2, C18 and C22 in Fig. 2 are generally less than 5° in all structures, with only two exceptions, the

most significant being the 9.5° Mo–Se2–C18–C22 torsion angle in the compound shown in Fig. 2.

The packing diagram of $[\text{Mo}(\text{CO})_4\{\text{FcSe}(\text{CH}_2)_3\text{SeFc}\}]$ is shown in Fig. 3. The compounds are monomeric, all with intermolecular contact distances in the normal ranges.

2.4. Comparison of ligand properties

As mentioned in the previous section, the equatorial M–C bonds *trans* to the Mo–E bonds are significantly shorter than the two axial Mo–C bonds. This results from greater back-bonding to the two equatorial carbonyls, and reflects the strength of the donor atom. Analysis of this and related effects allows comparison of the ferrocenyl chalcogenide ligands' properties.

Carbon monoxide behaves as a σ -donor and a π -acceptor. Strong σ -donor ligands attached to a mixed-ligand metal carbonyl, or a formal negative charge on a metal carbonyl anion, will increase the electron density on the metal atom. Then back-bonding induces a filling of the carbonyl π^* level, which causes a weakening of the C–O bond. This weakening is reflected both in the infrared spectrum and in the structure.

The number and intensities of carbonyl stretching bands in the vibrational spectra of carbonyl complexes depend on the local

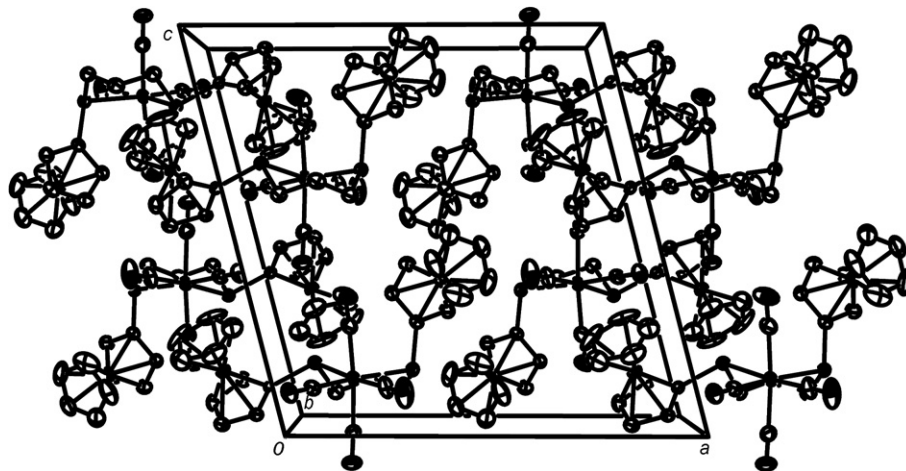


Fig. 3. Packing diagram for $[\text{Mo}(\text{CO})_4\{\text{FcSe}(\text{CH}_2)_3\text{SeFc}\}]$. Hydrogen atoms are omitted for clarity.

Table 2

IR spectroscopic data for $[\text{M}(\text{CO})_4\{\text{FcE}(\text{CH}_2)_3\text{E}'\text{Fc}\}]$ (M = Cr or W, E = E' = Te; M = Mo, E and E' = Se or Te)

Complex	$\nu(\text{CO}) \text{ cm}^{-1}$
$[\text{Cr}(\text{CO})_4\{\text{FcTe}(\text{CH}_2)_3\text{TeFc}\}]$	1995, 1908, 1877, 1846
$[\text{Mo}(\text{CO})_4\{\text{FcSe}(\text{CH}_2)_3\text{SeFc}\}]$	2018, 1912 (sh), 1879, 1841
$[\text{Mo}(\text{CO})_4\{\text{FcTe}(\text{CH}_2)_3\text{TeFc}\}]$	2015, 1914, 1881, 1843 (sh)
$[\text{Mo}(\text{CO})_4\{\text{FcTe}(\text{CH}_2)_3\text{TeFc}\}]$	2012, 1917, 1884, 1849 (sh)
$[\text{W}(\text{CO})_4\{\text{FcTe}(\text{CH}_2)_3\text{TeFc}\}]$	2006, 1908, 1874, 1841 (sh)

symmetry around the central atom; the expected number of IR-active bands can be derived from group theory. For a disubstituted octahedral complex $[\text{M}(\text{CO})_4\text{L}_2]$, there should be one IR active mode (E_u) for the *trans* isomer and four such modes ($2A_1 + B_1 + B_2$) for the *cis* one (the same is true of the less symmetric $[\text{M}(\text{CO})_4\text{LL}']$ complexes, and for convenience the same symmetry labels will be used for the vibrational modes in this case). The IR spectra of the *cis*- $[\text{M}(\text{CO})_4\{\text{FcE}(\text{CH}_2)_3\text{E}'\text{Fc}\}]$ complexes show four $\nu(\text{CO})$ bands as expected (Table 2). For the Mo complexes, the frequency of the highest A_1 mode falls with a change in donor from Se to Te: 2018 cm^{-1} , $[\text{Mo}(\text{CO})_4\{\text{FcSe}(\text{CH}_2)_3\text{SeFc}\}]$; 2015 cm^{-1} , $[\text{Mo}(\text{CO})_4\{\text{FcSe}(\text{CH}_2)_3\text{TeFc}\}]$; 2012 cm^{-1} , $[\text{Mo}(\text{CO})_4\{\text{FcTe}(\text{CH}_2)_3\text{TeFc}\}]$. This reflects the weakening of the C–O bond: the tellurium ligand places greater electron density on the metal centre resulting in greater π -back-bonding to CO. The C–O bond lengths confirm this interpretation: those which are *trans* to the donor ligand are slightly longer in $[\text{Mo}(\text{CO})_4\{\text{FcTe}(\text{CH}_2)_3\text{TeFc}\}]$ (1.155(5) and 1.156(5) Å) and $[\text{Mo}(\text{CO})_4\{\text{FcSe}(\text{CH}_2)_3\text{TeFc}\}]$ (1.156(6) and 1.153(5) Å) than in $[\text{Mo}(\text{CO})_4\{\text{FcSe}(\text{CH}_2)_3\text{SeFc}\}]$ (1.143(5) and 1.147(5) Å). Comparing the complexes of the same ligand FcTe(CH₂)₃TeFc, the frequency of the A_1 mode falls in the sequence Mo > W > Cr.

More information can be obtained from comparison of the structural data for the equatorial and axial carbonyls. As already noted, the equatorial M–C bonds *trans* to the M–E bonds (M–C(3) and M–C(4)) are significantly shorter than the two axial M–C bonds (M–C(1) and M–C(2)), as increased back-bonding strengthens the M–C bond, while inducing the weakening of the C–O bond. The C(3)–O(3) and C(4)–O(4) bonds are thus longer than the other two. For example, in $[\text{Mo}(\text{CO})_4\{\text{FcTe}(\text{CH}_2)_3\text{TeFc}\}]$ the Mo–C(3) and Mo–C(4) bonds are 1.943(5) and 1.969(4) Å respectively, shorter than Mo–C(1) and Mo–C(2) (2.009(5) and 2.041(5) Å), but the C(3)–O(3) and C(4)–O(4) bonds (1.155(5) and 1.156(5) Å) are slightly longer than C(1)–O(1) and C(2)–O(2) (1.146(5) and 1.143(5) Å). The same trends have been found for other molybdenum tetracarbonyls having two Se [17] or Te atoms [18] as additional donors.

For the three complexes of the same ligand, FcTe(CH₂)₃TeFc, the *trans*-C–O bond lengths appear to vary according to the sequence Cr > W ~ Mo: $[\text{Cr}(\text{CO})_4\{\text{FcTe}(\text{CH}_2)_3\text{TeFc}\}]$, 1.160(6) and 1.157(5) Å; $[\text{W}(\text{CO})_4\{\text{FcTe}(\text{CH}_2)_3\text{TeFc}\}]$, 1.157(7) and 1.153(6) Å; $[\text{Mo}(\text{CO})_4\{\text{FcTe}(\text{CH}_2)_3\text{TeFc}\}]$, 1.155(5) and 1.156(5) Å. This trend substantially mirrors what is observed in the IR spectra. Both effects may be ascribed to a change in electron density on the metal, which might be reflected in the stability of the complexes towards air oxidation:

Table 3

Cyclic voltammetric data, $E_{1/2}(|E_{pa} - E_{pc}|)$ (mV), for $[\text{M}(\text{CO})_4\{\text{FcE}(\text{CH}_2)_3\text{E}'\text{Fc}\}]^a$ (M = Cr or W, E = E' = Te; M = Mo, E and E' = Se or Te)

	E = E' = Se	E = Se; E' = Te	E = E' = Te
Cr	–	–	181 (218)
Mo	30 (151), 242 (184)	214 (225)	172 (184)
W	–	–	264 (208)

^a $E_{1/2}$ values are quoted relative to FcH/[FcH]⁺.

$[\text{Cr}(\text{CO})_4\{\text{FcTe}(\text{CH}_2)_3\text{TeFc}\}]$ is the least stable of those which could be isolated.

2.5. Electrochemistry

Cyclic voltammetry (supplemented by differential pulse voltammetry where appropriate) was used to investigate the electrochemistry of the complexes in dichloromethane solution, and the half-wave potentials ($E_{1/2}$) obtained are summarised in Table 3.

The chromium complex $[\text{Cr}(\text{CO})_4\{\text{FcTe}(\text{CH}_2)_3\text{TeFc}\}]$ exhibits two redox processes at 181 and 322 mV. We assign only the first process to ferrocene oxidation, as the second one can be attributed to the Cr(0)/Cr(I) couple. We have previously shown that in the system $[\text{M}\{\text{FcE}(\text{CH}_2)_3\text{E}'\text{Fc}\}_2(\text{PF}_6)_2$ (M = Pd, Pt; E, E' = Se, Te; Fc = $[\text{Fe}(\eta^5\text{-C}_5\text{H}_5)(\eta^5\text{-C}_5\text{H}_4)]$), communication between the ferrocenyl groups occurs by a “through bond” mechanism, with the threshold Fe···Fe distance in the range 13.17–13.37 Å [2]. From the crystal data, the through-bond Fe···Fe distance in $[\text{Cr}(\text{CO})_4\{\text{FcTe}(\text{CH}_2)_3\text{TeFc}\}]$ is 13.56 Å, which is beyond the communication threshold, assuming that it also applies in this case.

The CV of $[\text{Mo}(\text{CO})_4\{\text{FcSe}(\text{CH}_2)_3\text{SeFc}\}]$ has two quasi-reversible waves at 30 and 242 mV and one irreversible wave at 517 mV. The first two waves can be assigned to the redox processes at the iron centres of the ferrocenes; the third irreversible one corresponds to the redox couple Mo(0)/Mo(I). The observation of two ferrocene-based waves shows that there is an interaction between the ferrocenyl groups, as expected on the basis of our previous results, since the through-bond Fe···Fe distance of 13.17 Å should be short enough for communication to occur. The difference between the two half wave potentials is 212 mV. Complex $[\text{Pd}\{\text{FcSe}(\text{CH}_2)_3\text{TeFc}\}_2(\text{PF}_6)_2$ has a similar through bond Fe···Fe distance (13.16 Å), but a $\Delta E_{1/2}$ of only 119 mV in acetonitrile. This difference emphasises the importance of the nature of the intervening atoms in determining the magnitude of the interaction between ferrocene groups. It is not only dependent on the distance between them. It may also be relevant that the dielectric constant of dichloromethane is 9, which is much lower than that of acetonitrile (38), and results in higher cell resistance [19].

The CV of $[\text{Mo}(\text{CO})_4\{\text{FcSe}(\text{CH}_2)_3\text{TeFc}\}]$ contains only one quasi-reversible wave centred on the ferrocene units with $E_{1/2} = 214 \text{ mV}$. The through-bond Fe···Fe distance is 13.56 Å, which as in $[\text{Cr}(\text{CO})_4\{\text{FcTe}(\text{CH}_2)_3\text{TeFc}\}]$ should be too long for communication. The irreversible wave assigned to Mo(0)/Mo(I) is at 487 mV. A similar result was obtained for $[\text{Mo}(\text{CO})_4\{\text{FcTe}(\text{CH}_2)_3\text{TeFc}\}]$ which has a through bond Fe···Fe distance of 13.85 Å, with $E_{1/2} = 172 \text{ mV}$ for the ferrocene-based oxidation. The irreversible wave due to Mo(0)/Mo(I) is at 436 mV. In these three complexes, the oxidation of Mo(0) shifts to a lower potential as the donor atoms change from Se to Te, meaning that the Mo becomes easier to oxidise. As Te is a better σ -donor atom than Se, so it will increase the electron density on the Mo, facilitating the oxidation process.

The through bond Fe···Fe distance is 13.84 Å in $[\text{W}(\text{CO})_4\{\text{FcTe}(\text{CH}_2)_3\text{TeFc}\}]$, and its CV only has one quasi-reversible wave due to the ferrocene units with $E_{1/2} = 264 \text{ mV}$. The irreversible wave centred on W was not resolved.

3. Conclusion

The Group 6 metal tetracarbonyl complexes $[\text{Cr}(\text{CO})_4\{\text{FcTe}(\text{CH}_2)_3\text{TeFc}\}]$, $[\text{Mo}(\text{CO})_4\{\text{FcE}(\text{CH}_2)_3\text{E}'\text{Fc}\}]$ (E = E' = Se; E = Se, E' = Te; E = E' = Te), and $[\text{W}(\text{CO})_4\{\text{FcTe}(\text{CH}_2)_3\text{TeFc}\}]$ (Fc = $[\text{Fe}(\eta^5\text{-C}_5\text{H}_5)(\eta^5\text{-C}_5\text{H}_4)]$) have been prepared and fully characterised. The spectroscopic and structural data obtained for these compounds show the effects of increased σ -donation on changing the donor atoms from Se to Te. Interaction between the ferrocenyl groups is ob-

served to follow the same pattern as in the Pd(II) and Pt(II) complexes of the same ligand set: beyond a threshold Fe···Fe distance of 13.17 Å there is no observable communication between them. Work to explore the generality of this conclusion is ongoing.

4. Experimental

4.1. Materials and general procedures

All the reactions were carried out under nitrogen using standard Schlenk techniques. All solvents used in the reactions were distilled over elemental alkali metal or Na/K alloy except ethanol (which was degassed before use) and dichloromethane (which was distilled over calcium hydride). Bis(ferrocenylchalcogeno)propanes, $\text{FcE}(\text{CH}_2)_3\text{E}'\text{Fc}$ (E, E' = Se or Te; Fc = ferrocenyl, $[\text{Fe}(\eta^5\text{-C}_5\text{H}_5)(\eta^5\text{-C}_5\text{H}_4)]$), were prepared following the previously reported method [1]. Group 6 metal tetracarbonyl precursors, $[\text{Cr}(\text{CO})_4(\text{nbd})]$, $[\text{Mo}(\text{CO})_4(\text{nbd})]$ (nbd = norbornadiene), and $[\text{W}(\text{CO})_4(\text{TMPDA})]$ (TMPDA = tetramethylpropylenediamine, 1,3-bis(dimethylamino)propane), were synthesised by literature procedures [20,21].

4.2. Physical measurements

^1H and ^{13}C NMR spectra were recorded on a Bruker AV400 spectrometer at 400.1 and 100.6 MHz, respectively, with tetramethylsilane as internal standard. ^{77}Se NMR Spectra were recorded at 47.7 MHz on a Bruker WM250 spectrometer, with dimethyl selenide as external standard. Chemical shifts (δ) are reported in ppm; J values are given in Hz. NMR spectra were recorded in freshly prepared CD_2Cl_2 solutions. As a result of slow decomposition, resonances due to the free ligand sometimes appeared in the ^{77}Se and ^{125}Te spectra of the complexes when recorded over a long timescale.

Elemental analyses were performed by the Warwick Analytical Service, University of Warwick Science Park, Coventry, UK. Mass spectra were recorded by the EPSRC Mass Spectrometry Centre, using fast atom bombardment (FAB); m/z values have been rounded to the nearest integer or half-integer. Assignments are based on isotopomers containing ^1H , ^{12}C , ^{16}O , ^{56}Fe , ^{80}Se , ^{130}Te , and ^{52}Cr , ^{98}Mo or ^{184}W ; expected isotope distribution patterns were observed. IR spectra were obtained on a Perkin-Elmer Spectrum One FT-IR Spectrometer. Cyclic voltammetry (CV) and differential pulse voltammetry (DPV) measurements were performed at room temperature in a dry dichloromethane solution containing 0.1 M $[\text{NBu}_4]\text{PF}_6$ electrolyte using an Autolab PGSTAT30 potentiostat system. The sweep rate was 100 mV s^{-1} (CV) or 72 mV s^{-1} (DPV). A three-electrode arrangement was used with a Pt working electrode, a Pt wire counter electrode and a Ag/Ag^+ (0.01 M AgNO_3 in CH_2Cl_2) reference electrode.

4.3. Syntheses

4.3.1. $[\text{Cr}(\text{CO})_4\{\text{FcTe}(\text{CH}_2)_3\text{TeFc}\}]$

$[\text{Cr}(\text{CO})_4(\text{nbd})]$ (120 mg, 0.47 mmol) was dissolved in degassed toluene (40 ml) and the ligand $\text{FcTe}(\text{CH}_2)_3\text{TeFc}$ (318 mg, 0.47 mmol) added. The reaction mixture was stirred at 100°C overnight and then the toluene removed *in vacuo*. The residue was dissolved in CH_2Cl_2 (5 ml), filtered and cold hexane added to yield a brown powder. The powder was collected, washed with cold hexane and dried under vacuum. Yield: 156 mg, 40%. Anal. Calc. for $\text{C}_{27}\text{H}_{24}\text{CrFe}_2\text{O}_4\text{Te}_2$ (831.38): C, 39.01; H, 2.91. Found: C, 36.26; H, 2.82%. ^1H NMR (CD_2Cl_2): 4.55 (C_5H_4 , H_{2+5} , br, 4H), 4.29 (C_5H_4 , H_{3+4} , m, 4H), 4.18 (C_5H_5 , m, 10H), 2.85 (TeCH_2 , br, 4H), 2.49 ($\text{CH}_2\text{CH}_2\text{CH}_2$, m, 4H). ^{13}C NMR (CD_2Cl_2): 207.6 (CO), 76.4, 76.3

(C_5H_4 , C_{2+5}), 72.7, 71.9 (C_5H_4 , C_{3+4}), 70.6 (C_5H_5), 47.1 (C_1), 26.3 ($\text{CH}_2\text{CH}_2\text{CH}_2$), 12.7 (TeCH_2 , $^1J_{\text{Te-C}} = 156.4\text{ Hz}$). ^{125}Te NMR (CD_2Cl_2): 429. FAB MS: 836 ($[\text{M}]^+$), 724 ($[\text{M}-4\text{CO}]^+$), 672 ($[\text{M}-\text{Cr}(\text{CO})_4]^+$).

4.3.2. $[\text{Mo}(\text{CO})_4\{\text{FcSe}(\text{CH}_2)_3\text{SeFc}\}]$

$[\text{Mo}(\text{CO})_4(\text{nbd})]$ (195 mg, 0.65 mmol) was dissolved in degassed toluene (40 ml) and the ligand $\text{FcSe}(\text{CH}_2)_3\text{SeFc}$ (369 mg, 0.65 mmol) added. The reaction mixture was stirred at room temperature overnight and then the toluene removed *in vacuo*. The residue was dissolved in CH_2Cl_2 (5 ml), filtered and cold hexane added to yield a brown powder. The powder was collected, washed with cold hexane and dried under vacuum. Yield: 156 mg, 31%. Anal. Calc. for $\text{C}_{27}\text{H}_{24}\text{Fe}_2\text{MoO}_4\text{Se}_2$ (778.04): C, 41.68; H, 3.11; satisfactory microanalysis could not be obtained. ^1H NMR (CD_2Cl_2): 5.24 (C_5H_4 , H_{2+5} , m, 4H), 4.27 (C_5H_4 , H_{3+4} , m, 4H), 4.25 (C_5H_5 , s, 10H), 2.80 (SeCH_2 , t, br, 4H), 1.88 ($\text{CH}_2\text{CH}_2\text{CH}_2$, m, br, 2H). ^{13}C NMR (CDCl_3): 217.7, 209.5 (CO), 76.0 (C_5H_4 , C_{2+5}), 71.0 (C_1), 70.4 (C_5H_4 , C_{3+4}), 70.0 (C_5H_5), 36.6 ($\text{CH}_2\text{CH}_2\text{CH}_2$), 27.2 (SeCH_2). ^{77}Se NMR (CDCl_3): 176. FAB MS: 782 ($[\text{M}]^+$), 572 ($[\text{M}-\text{Mo}(\text{CO})_4]^+$).

4.3.3. $[\text{Mo}(\text{CO})_4\{\text{FcSe}(\text{CH}_2)_3\text{TeFc}\}]$

Method as for $[\text{Mo}(\text{CO})_4\{\text{FcSe}(\text{CH}_2)_3\text{SeFc}\}]$, yield: 80%. Anal. Calc. for $\text{C}_{27}\text{H}_{24}\text{Fe}_2\text{MoO}_4\text{SeTe}$ (826.68): C, 39.23; H, 2.93. Found: C, 38.79; H, 2.89%. ^1H NMR (CD_2Cl_2): 4.57, 4.47 (C_5H_4 , H_{2+5} , br, 4H), 4.37, 4.31 (C_5H_4 , H_{3+4} , br, 4H), 4.23, 4.20 (C_5H_5 , s, 10H), 2.77, 2.55 (SeCH_2 , TeCH_2 , br, 4H), 1.99–1.80 ($\text{CH}_2\text{CH}_2\text{CH}_2$, m, 2H). ^{13}C NMR (CD_2Cl_2): 217.8, 216.2, 210.9, 206.9 (CO), 77.8, 77.5, 76.7, 76.2 (C_5H_4 , C_{2+5}), 74.0, 73.0, 71.9, 71.3 (C_5H_4 , C_{3+4}), 70.7, 70.5, 70.3 (C_5H_5), 38.2 (TeC_1), 31.9, 30.9, 30.6 ($\text{CH}_2\text{CH}_2\text{CH}_2$), 27.8 (SeCH_2), 17.7, 12.7 (TeCH_2). ^{77}Se NMR (CD_2Cl_2): 175. ^{125}Te NMR (CD_2Cl_2): 337. FAB MS: 832 ($[\text{M}]^+$).

4.3.4. $[\text{Mo}(\text{CO})_4\{\text{FcTe}(\text{CH}_2)_3\text{TeFc}\}]$

Method as for $[\text{Mo}(\text{CO})_4\{\text{FcSe}(\text{CH}_2)_3\text{SeFc}\}]$, yield: 60%. Anal. Calc. for $\text{C}_{27}\text{H}_{24}\text{Fe}_2\text{MoO}_4\text{Te}_2$ (875.32): C, 37.05; H, 2.76. Found: C, 36.72; H, 2.76%. ^1H NMR (CD_2Cl_2): 4.53, 4.50 (C_5H_4 , H_{2+5} , m, 4H), 4.33, 4.28 (C_5H_4 , H_{3+4} , m, 4H), 4.18 (C_5H_5 , s, 10H), 2.61, 2.43 (TeCH_2 , m, 4H), 1.66 ($\text{CH}_2\text{CH}_2\text{CH}_2$, m, 2H). ^{13}C NMR (CD_2Cl_2): 216.6, 211.7 (CO), 73.0 (C_5H_4 , C_{2+5}), 71.5 (C_5H_4 , C_{3+4}), 70.6 (C_5H_5), 47.6 (C_1), 27.5 ($\text{CH}_2\text{CH}_2\text{CH}_2$), 13.8 (TeCH_2). ^{125}Te NMR (CD_2Cl_2): 344. FAB MS: 882 ($[\text{M}]^+$).

4.3.5. $[\text{W}(\text{CO})_4\{\text{FcTe}(\text{CH}_2)_3\text{TeFc}\}]$

$[\text{W}(\text{CO})_4(\text{TMPDA})]$ (146 mg, 0.34 mmol) was dissolved in degassed toluene (40 ml) and the ligand $\text{FcTe}(\text{CH}_2)_3\text{TeFc}$ (230 mg, 0.34 mmol) added. The reaction mixture was stirred at 80°C overnight and then the toluene removed *in vacuo*. The residue was dissolved in CH_2Cl_2 (5 ml), filtered and cold hexane added to yield a brown powder. The powder was collected, washed with cold hexane and dried under vacuum. Yield 173 mg, 53%. Anal. Calc. for $\text{C}_{27}\text{H}_{24}\text{Fe}_2\text{O}_4\text{Te}_2\text{W}$ (963.23): C, 33.67; H, 2.51. Found: C, 35.99; H, 3.04%. ^1H NMR (CD_2Cl_2): 4.42 (C_5H_4 , H_{2+5} , m, 4H), 4.17 (C_5H_4 , H_{3+4} , m, 4H), 4.05 (C_5H_5 , s, 10H), 2.65 (TeCH_2 , t, 4H, $^3J_{\text{H-H}} = 9\text{ Hz}$), 1.71 ($\text{CH}_2\text{CH}_2\text{CH}_2$, m, 2H). ^{13}C NMR (CD_2Cl_2): 204.7, 202.7 (CO), 77.6 (C_5H_4 , C_{2+5}), 69.9 (C_5H_4 , C_{3+4}), 68.6 (C_5H_5), 47.0 (C_1), 28.9 ($\text{CH}_2\text{CH}_2\text{CH}_2$), 12.9 (TeCH_2). ^{125}Te NMR (CD_2Cl_2): 272 ($^1J_{\text{Te-W}} = 74\text{ Hz}$), 269. FAB MS: 968 ($[\text{M}]^+$), 940 ($[\text{M}-\text{CO}]^+$), 856 ($[\text{M}-4\text{CO}]^+$), 672 ($[\text{M}-\text{W}(\text{CO})_4]^+$).

4.4. X-ray crystallography

Crystals of $[\text{Cr}(\text{CO})_4\{\text{FcTe}(\text{CH}_2)_3\text{TeFc}\}]$, $[\text{Mo}(\text{CO})_4\{\text{FcE}(\text{CH}_2)_3\text{E}'\text{Fc}\}]$ (E = E' = Se; E = Se, E' = Te; E = E' = Te), and $[\text{W}(\text{CO})_4\{\text{FcTe}(\text{CH}_2)_3\text{TeFc}\}]$ were obtained from CH_2Cl_2 /hexanes. X-ray diffraction data were collected at room temperature on an Oxford Diffraction Xcalibur 3 CCD diffractometer, using Mo $K\alpha$

Table 4Crystallographic data and collection and refinement parameters of $[\text{M}(\text{CO})_4\{\text{FcTe}(\text{CH}_2)_3\text{TeFc}\}]$ (M = Cr or W)

Compound	$[\text{Cr}(\text{CO})_4\{\text{FcTe}(\text{CH}_2)_3\text{TeFc}\}]$	$[\text{W}(\text{CO})_4\{\text{FcTe}(\text{CH}_2)_3\text{TeFc}\}]$
Empirical formula	$\text{C}_{27}\text{H}_{24}\text{CrFe}_2\text{O}_4\text{Te}_2$	$\text{C}_{27}\text{H}_{24}\text{Fe}_2\text{WO}_4\text{Te}_2$
Formula weight	831.36	963.21
<i>T</i> (K)	293(2)	293(2)
Wavelength (Å)	0.71069	0.71069
Crystal system	Monoclinic	Monoclinic
Space group	$P2_1/c$	$P2_1/c$
<i>a</i> (Å)	15.186(1)	15.254(1)
<i>b</i> (Å)	12.369(1)	12.476(1)
<i>c</i> (Å)	15.335(1)	15.396(1)
α (°)	90	90
β (°)	103.55(1)	103.19(1)
γ (°)	90	90
Volume (Å ³)	2800.3(3)	2852.7(3)
<i>Z</i>	4	4
<i>D_c</i> (Mg m ⁻³)	1.972	2.243
Absorption coefficient (mm ⁻¹)	3.476	7.061
<i>F</i> (000)	1592	1792
Crystal size (mm)	0.40 × 0.40 × 0.25	0.30 × 0.20 × 0.15
θ Range for data collection (°)	4.30–26.37	4.25–26.37
Reflections collected	27 434	28 246
Independent reflections [<i>R</i> _{int}]	5680 [0.0356]	5803 [0.0339]
Data/restraints/parameters	5680/0/325	5803/0/326
Goodness-of-fit on <i>F</i> ²	1.015	0.977
Final <i>R</i> indices [<i>I</i> > 2σ(<i>I</i>)]	<i>R</i> ₁ = 0.0335, <i>wR</i> ₂ = 0.0776	<i>R</i> ₁ = 0.0305, <i>wR</i> ₂ = 0.0656
<i>R</i> indices (all data)	<i>R</i> ₁ = 0.0436, <i>wR</i> ₂ = 0.0813	<i>R</i> ₁ = 0.0428, <i>wR</i> ₂ = 0.0688
Largest difference in peak and hole (e Å ⁻³)	1.341, −0.73	1.181, −0.828

radiation ($\lambda = 0.71069$ Å). Crystal data, data collection parameters and analysis statistics are summarised in Table 4 ($[\text{Cr}(\text{CO})_4\{\text{FcTe}(\text{CH}_2)_3\text{TeFc}\}]$ and $[\text{W}(\text{CO})_4\{\text{FcTe}(\text{CH}_2)_3\text{TeFc}\}]$) and Table 5 ($[\text{Mo}(\text{CO})_4\{\text{FcE}(\text{CH}_2)_3\text{E'Fc}\}]$; E = E' = Se; E = Se, E' = Te; E = E' = Te). Corrections for absorption were applied with SADABS [22]. The compounds are isomorphous and crystallize in the monoclinic system, as revealed by the symmetry of their diffraction patterns, in spite

of a pseudo-orthorhombic metric of the lattice. The structure of $[\text{Mo}(\text{CO})_4\{\text{FcSe}(\text{CH}_2)_3\text{SeFc}\}]$ was determined by direct methods, with SIR-97 [23] and that of $[\text{Mo}(\text{CO})_4\{\text{FcSe}(\text{CH}_2)_3\text{TeFc}\}]$ was solved with SHELXS-97 [24]; both models were completed by series of difference Fourier. The structure of $[\text{Mo}(\text{CO})_4\{\text{FcSe}(\text{CH}_2)_3\text{TeFc}\}]$ was found to be affected by orientational disorder of the ligand, which resulted in fractional occupancies of the coordination sites by the Se and Te atoms, whose complementary population parameters were refined (0.408(3) (Se) and 0.592(3) (Te) are the final values for the site having higher Te occupancy), while the positional and thermal parameters were constrained to be identical. The $[\text{Mo}(\text{CO})_4\{\text{FcSe}(\text{CH}_2)_3\text{SeFc}\}]$ model provided the initial geometries for the remaining three isomorphous compounds, with due consideration of the changes in the nature of the chalcogen atoms. In the full-matrix least-squares refinement, based on *F*² values, SHELXL-97 was employed [25]. In the final cycles the non-hydrogen atoms were refined anisotropically and hydrogens were placed in idealized positions, each riding on the respective carrier atom, with $U_{\text{H}} = 1.2U_{\text{C}}^{\text{eq}}$. Residual features in the final difference density maps were generally close to the heavy-atom positions and had no chemical meaning. Other programs used in the crystallographic calculations included PARST for analysis of geometries [26], and ORTEP for graphics [27].

Acknowledgements

We thank the University of Wales Swansea and University of Wales Swansea/China Scholarship Council for the provision of research studentships to C.A.W. and S.J. respectively, and the Ministero dell' Università e della Ricerca Scientifica e Tecnologica for financial support to M. di V.

Appendix A. Supplementary material

CCDC 675281, 675282, 675283, 675284 and 675285 contain the supplementary crystallographic data for this paper. These data can be obtained free of charge from The Cambridge Crystallographic Data Centre via www.ccdc.cam.ac.uk/data_request/cif. Supplement-

Table 5Crystallographic data and collection and refinement parameters of $[\text{Mo}(\text{CO})_4\{\text{FcE}(\text{CH}_2)_3\text{E'Fc}\}]$ (E and E' = Se or Te)

Compound	$[\text{Mo}(\text{CO})_4\{\text{FcSe}(\text{CH}_2)_3\text{SeFc}\}]$	$[\text{Mo}(\text{CO})_4\{\text{FcSe}(\text{CH}_2)_3\text{TeFc}\}]$	$[\text{Mo}(\text{CO})_4\{\text{FcTe}(\text{CH}_2)_3\text{TeFc}\}]$
Empirical formula	$\text{C}_{27}\text{H}_{24}\text{Fe}_2\text{MoO}_4\text{Se}_2$	$\text{C}_{27}\text{H}_{24}\text{Fe}_2\text{MoO}_4\text{SeTe}$	$\text{C}_{27}\text{H}_{24}\text{Fe}_2\text{MoO}_4\text{Te}_2$
Formula weight	778.02	826.66	875.30
<i>T</i> (K)	293(2)	293(2)	293(2)
Wavelength (Å)	0.71069	0.71069	0.71069
Crystal system	Monoclinic	Monoclinic	Monoclinic
Space group	$P2_1/c$	$P2_1/c$	$P2_1/c$
<i>a</i> (Å)	15.030(3)	15.1636(8)	15.253(5)
<i>b</i> (Å)	12.468(3)	12.5154(6)	12.512(4)
<i>c</i> (Å)	15.066(3)	15.2988(8)	15.411(5)
α (°)	90	90	90
β (°)	104.46(2)	103.680(5)	103.14(3)
γ (°)	90	90	90
Volume (Å ³)	2733.8(10)	2821.0(2)	2864.1(16)
<i>Z</i>	4	4	4
<i>D_c</i> (Mg m ⁻³)	1.890	1.946	2.030
Absorption coefficient (mm ⁻¹)	4.193	3.787	3.457
<i>F</i> (000)	1520	1592	1664
Crystal size (mm)	0.60 × 0.50 × 0.30	0.35 × 0.25 × 0.15	0.40 × 0.35 × 0.30
θ Range for data collection (°)	4.42–26.02	4.26–25.68	4.24–28.28
Reflections collected	12 969	23 118	30 720
Independent reflections [<i>R</i> _{int}]	5330 [0.0499]	5325 [0.0278]	7049 [0.0421]
Data/restraints/parameters	5330/0/326	5325/0/326	7049/0/326
Goodness-of-fit on <i>F</i> ²	0.832	1.038	0.960
Final <i>R</i> indices [<i>I</i> > 2σ(<i>I</i>)]	<i>R</i> ₁ = 0.0320, <i>wR</i> ₂ = 0.0600	<i>R</i> ₁ = 0.0331, <i>wR</i> ₂ = 0.0827	<i>R</i> ₁ = 0.0342, <i>wR</i> ₂ = 0.0740
<i>R</i> indices (all data)	<i>R</i> ₁ = 0.0522, <i>wR</i> ₂ = 0.0634	<i>R</i> ₁ = 0.0444, <i>wR</i> ₂ = 0.0874	<i>R</i> ₁ = 0.0513, <i>wR</i> ₂ = 0.0791
Largest difference in peak and hole (e Å ⁻³)	0.608, −0.718	1.145, −0.522	0.963, −0.734

tary data associated with this article can be found, in the online version, at doi:10.1016/j.jorganchem.2008.04.004.

References

- [1] M.R. Burgess, S. Jing, C.P. Morley, J. Organomet. Chem. 691 (2006) 3484.
- [2] S. Jing, C.P. Morley, C.A. Webster, M. Di Vaira, Dalton Trans. (2006) 4335.
- [3] E.W. Abel, G.V. Hutson, J. Inorg. Nucl. Chem. 31 (1969) 3333.
- [4] G. Hunter, R.C. Massey, J. Chem. Soc., Dalton Trans. (1976) 2007.
- [5] R. Donaldson, G. Hunter, R.C. Massey, J. Chem. Soc., Dalton Trans. (1974) 288.
- [6] G. Hunter, R.C. Massey, J. Chem. Soc., Dalton Trans. (1975) 209.
- [7] E.W. Abel, N.J. Long, K.G. Orrell, A.G. Osborne, V. Sik, P.A. Bates, M.B. Hursthouse, J. Organomet. Chem. 367 (1989) 275.
- [8] E.W. Abel, N.J. Long, K.G. Orrell, A.G. Osborne, V. Sik, P.A. Bates, M.B. Hursthouse, J. Organomet. Chem. 383 (1990) 253.
- [9] E.W. Abel, N.J. Long, K.G. Orrell, A.G. Osborne, V. Sik, J. Organomet. Chem. 378 (1989) 473.
- [10] R. Kaur, H.B. Singh, R.J. Butcher, Organometallics 14 (1995) 4755.
- [11] A.J. Barton, W. Levason, G. Reid, J. Organomet. Chem. 579 (1999) 235.
- [12] W. Levason, B. Patel, G. Reid, A.J. Ward, J. Organomet. Chem. 619 (2001) 218.
- [13] A.J. Barton, J. Connolly, W. Levason, A. Media-Jalon, S.D. Orchard, G. Reid, Polyhedron 19 (2000) 1373.
- [14] M.K. Davis, M.C. Durrant, W. Levason, G. Reid, R.L. Richards, J. Chem. Soc., Dalton Trans. (1999) 1077.
- [15] W. Levason, S.D. Orchard, G. Reid, Organometallics 18 (1999) 1275.
- [16] E.W. Abel, S.K. Bhargava, K.G. Orrell, Prog. Inorg. Chem. 32 (1984) 1.
- [17] H. Herberhold, G.-Z. Jin, A.L. Rheingold, J. Organomet. Chem. 570 (1998) 241.
- [18] W. Levason, G. Reid, V.-A. Tolhurst, J. Chem. Soc., Dalton Trans. (1998) 3411.
- [19] J.B. Headridge, Electrochemical Techniques for Inorganic Chemists, Academic Press, USA, 1969.
- [20] J.J. Eisch, R.B. King, Organomet. Syn. 1 (1965) 122.
- [21] G.R. Dobson, G.C. Faber, Inorg. Chim. Acta 4 (1970) 87.
- [22] G.M. Sheldrick, SADABS, Program for Empirical Absorption Corrections, University of Göttingen, Göttingen, Germany, 1986.
- [23] A. Altomare, M.C. Burla, M. Camalli, G. Cascarano, C. Giacovazzo, A. Guagliardi, A.G. Moliterni, G. Polidori, R. Spagna, J. Appl. Crystallogr. 32 (1999) 115.
- [24] G.M. Sheldrick, SHELXS-97, Program for Automatic Solution of Crystal Structures, University of Göttingen, Göttingen, Germany, 1997.
- [25] G.M. Sheldrick, SHELXL-97, Program for Crystal Structure Refinement, University of Göttingen, Göttingen, Germany, 1997.
- [26] M. Nardelli, J. Appl. Crystallogr. 28 (1995) 659.
- [27] L.J. Farrugia, J. Appl. Crystallogr. 30 (1997) 565.